

# Design and Performance Investigation of Symmetrical Dual Gate Doping-less TFET for Biomolecule Recognition

Ms. Aishwarya Tomar, Dr. AK Shankhwar\*

ECE Deptt., HBTU, Kanpur, Uttar Pradesh, India

\*Corresponding author

doi: <https://doi.org/10.21467/proceedings.114.72>

## Abstract

This manuscript presents a dielectric modulated doping-less dual metal Gate Tunnel Field Effect Transistor (DL-DMG-TFET) sensor. In which a nano-cavity is presented above the tunnelling point to recognize the bio-molecule like amino acids (AAs), protein, and so on the proposed P+ and N+ sections are invented relying on the electrode's work-function on silicon body. The impacts of metal work regulation, cavity length and thickness variety are investigated for improving band-to-band tunnelling probability at the source-channel intersection. The proposed structure shows perceptible affectability results for neutral and charged biomolecules. The sensitivity of the higher dielectric constant bio-molecules are higher as compared to bio-molecule having lower dielectric constant; the drain current sensitivity of the Gelatin ( $k=12$ ) is assessed as  $3 \times 10^{10}$  which is 13% and 35% higher than the affectability of Keratin ( $k=10$ ) and Bacteriophage T7 ( $k=5$ ) separately at the nano-cavity length of 30 nm.

**Keywords:** Charged Plasma, Dielectric Constant, Tunnel Field Effect Transistor (TFET), Dual Gate (DG), Neutral Biomolecule.

## 1 Introduction

The miniaturization of MOSFETs has continued for the past couple of years and went to the nano-scale framework. Regardless, supply voltage ( $V_{DD}$ ) and leakage current has not reduced concerning the decline in real measurements. Certain components limit this downsizing. These elements are such as short channel impacts and subthreshold swing (SS) [1-4]. The conduction phenomenon utilized by MOSFET follows the system known as thermionic emission through which the subthreshold swing (SS) becomes temperature subordinate. This temperature dependence makes the subthreshold swing factor non-adaptable under its lower limit, which is set at 60mv/decade at room temperature.

The advantages of TFET show its utility as a very low power device in the near future. Nonetheless, a couple of issues remain questionable which limit the introduction and utility of TFETs. Some huge ones among them remember the low drive current ( $I_{ON}$ ) when appeared differently in relation to ordinary MOSFETs and high ambipolarity (conduction for both positive and negative entryway voltages) [5-7].

A couple of techniques are familiar in later quite a while with improving the  $I_{ON}$  of device-like usage of small bandgap materials, gate oxide having higher  $k$ -dielectric, heterostructure and nanowire TFET [2], [6-8]. To deal with ambipolar current concern, various strategies had been introduced in earlier years like higher bandgap material on drain end, underlapped drain side, overlapping gate terminal on channel using a low drain doping profile and dual material electrode [7].

Another appalling quality of TFETs is the essentiality of sharp convergences for capable BTBT [9], [10]. This orders a high thermal budget in case of doped source/channel due to thermal annealing and implantation technique [8-10]. For doped devices, diffusion of charge carriers to the channel section from drain (or source) region makes an abrupt interface profile hard to achieve. Similarly, with an interminable



reduction in size of doped TFET having high doping profile achieves higher random dopant fluctuations (RDF) causing variability in output characteristics [9-12]. The charge plasma procedure for making n-type or p-type sections in TFET without doping (Doping-Less TFET) is familiar with defeating this issue [13]. Metal electrodes having sensible work has been used to obtain n-type or p-type regions on intrinsic material body in charge plasma procedure.

Biosensors are biorecognition devices that recognize the target biomolecule [8-12]. Conventional FET has demonstrated inefficient to give required accomplishment in the nanoscale region. There are diverse nanoscale structures previously proposed for a low power device. From the innovation development point of view, we have picked dielectric modulated doping-less dual metal Gate Tunnel Field Effect Transistor (DL-DMG-TFET) sensor, which has high Ion/Ioff current proportion, low leakage current [14-17] and more extreme subthreshold slope when contrasted with the MOSFET. This paper reasons that an all-encompassing number of gate electrodes in the proposed design can improve the electrostatic control of the channel, which can diminish SCEs [18-21].

## **2 Proposed Device Structure**

Fig. 1 depicts conventional dopingless TFET, dielectric modulated doping-less dual metal Gate Tunnel Field Effect Transistor (DL-DMG-TFET) sensor, and the experimented ON current characteristic. The p type and n type districts are shaped on Si substrate, having a thickness of 10 nm. The intrinsic carrier concentration of silicon substrate is taken as,  $n_i = 1 \times 10^{15} \text{ cm}^{-3}$  For uniformly inducing carrier concentration alongside the silicon thickness, the substrate width is set aside underneath the Debye length  $((\epsilon_{\text{Si}} * V_T)/q + 60 * n)^{1/2}$ , where  $V_T$  means thermal voltage and  $n$  signifies the carrier concentration in the substrate,  $\epsilon_{\text{Si}}$  indicates dielectric value of silicon and  $q$  signifies elementary charge [13].

When the silicon substrate width is above 10 nm, the quantum mechanical effects have not been checked [34]. Platinum metal is used for concocting 'P+' source zone as metal terminal (work assessment of 5.93 eV). Furthermore, for imagining 'N+' region hafnium metal terminal with work assessment of 3.9 eV is used [17], [18]. Silicon dioxide (0.5nm thick) is embedded between the source metal terminal and silicon substrate to prevent silicide development. The oxide spacer of 15 nm has been taken between channel electrode and gate electrode (LS2). The gate terminal is divided into two metal electrodes - (i) the corner cathode close to source (G1), (ii) the corner electrode close to drain (G2) as depicted in Fig. 1.

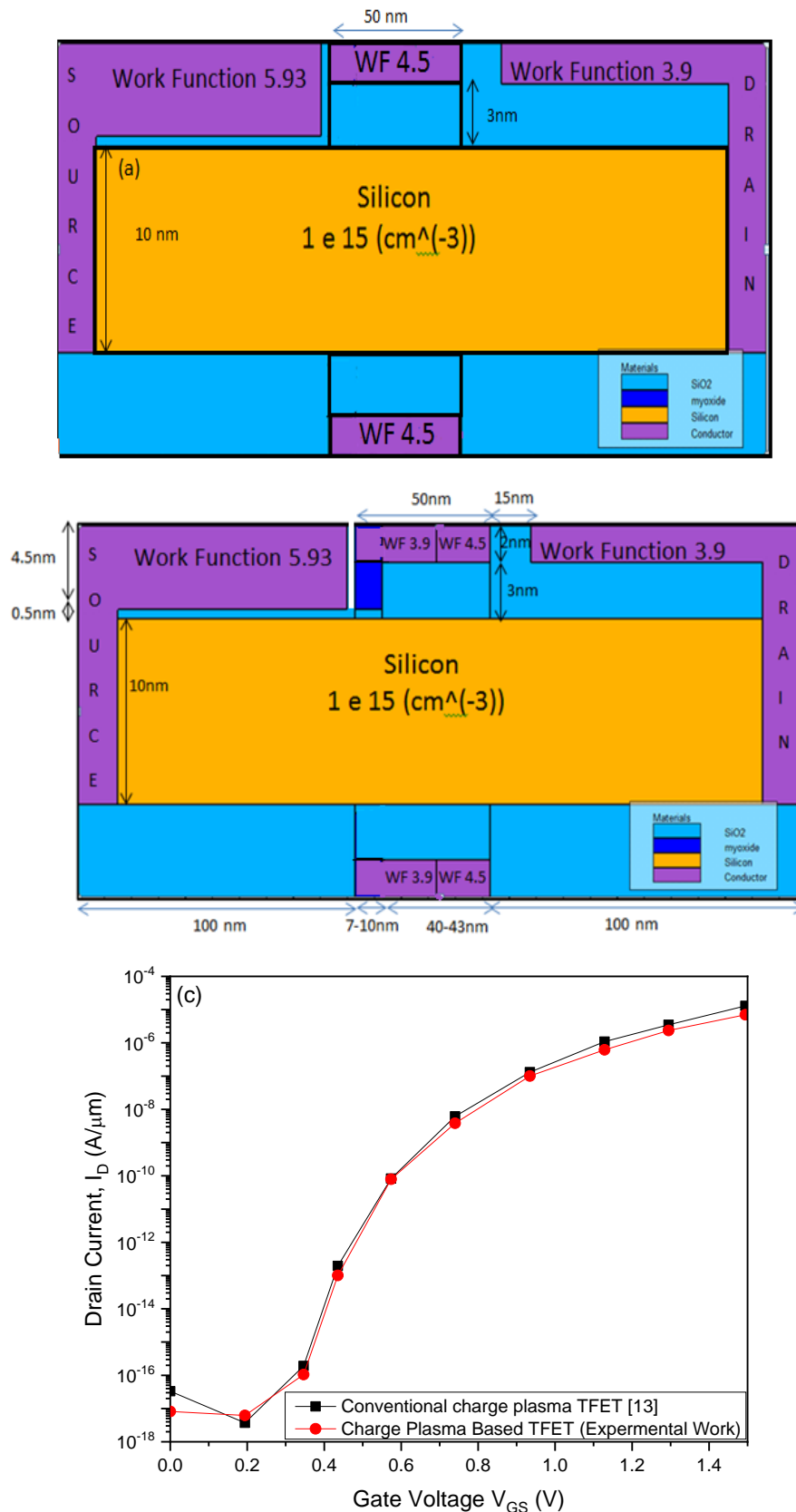


Fig.1. Cross-sectional view of a) Conventional charge plasma TFET, b) dielectric modulated doping-less dual metal Gate Tunnel Field Effect Transistor (DL-DMG-TFET) sensor device c) Experimented characteristics of charge plasma based TFET structure simulated output current with conventional doping-less TFET.

Models utilized in the recreation of dielectric modulated doping-less dual metal Gate Tunnel Field Effect Transistor (DL-DMG-TFET) sensor is Fermi–Dirac, CVT model, and for recombination SRH model and band to band tunneling model. The charge plasma idea and dual material electrode with the streamlined construction is utilized to drop down random dopant fluctuation and short channel impact, in additionally improve  $I_{ON}$  current. The effect of change in permittivity and surface charge density is completely investigated through potential,  $I_{ON}$  curve and its sensitivity curve. The device value used for simulation of the proposed dielectric modulated doping-less dual metal gate Tunnel Field Effect Transistor (DL-DMG-TFET) sensor is determined in Table I.

TABLE I. DEVICE VALUE OF CPB-TG-TFET

Parameters	Values
Channel length ( $L_C$ )	50 nm
Silicon substrate width ( $T_{Si}$ )	10 nm
Channel doping	$1 \times 10^{15} \text{ cm}^{-3}$
Gate oxide thickness	$\text{SiO}_2$ (3 nm)
Spacer thickness ( $L_S$ and $L_D$ )	3nm and 15nm
Gate1, Gate2 and Gate3 length	25nm, 15nm and 10nm
Work function of Gate1 ( $M1$ ) and Gate2 ( $M2$ )	3.9 eV and 4.5 eV
Cavity thickness ( $T_{cav}$ )	2.5 nm
Cavity length ( $L_{cav}$ )	8-10 nm

**Calibration characteristic:** The simulated outcome of conventional doping-less TFET following the reported work in [13] is depicted in Figure 1(c). True experimental data have been found by applying a Plot Digitizer tool.

### 3 Results and Discussions

The n-type dielectric modulated doping-less dual metal Gate Tunnel Field Effect Transistor (DL-DMG-TFET) sensor which is explored in this paper has been simulated by utilizing the Atlas [15] tool. Hence, the specific biological molecules are coordinated with the dielectric constant of the occupied material in the nanogap to recognize the biological molecules confined in the nanogap; like relative permittivity  $K=6$  corresponds to Bacteriophage T7 and  $K=12$  shows the identity of Gelatin. Here,  $k=6$  (Bacteriophage T7) and  $k=12$  (Gelatin) is utilized for the simulation and their sensitivities are obtained by examining the electrostatic property of the device. The efficiency of biosensors is assessed by acknowledging ON current sensitivity as follows:

Sensitivity of drain current can be found out by using formula mentioned below:

$$\Psi_{\text{drain current}}(\%) = \left[ \left( \frac{(\Psi_{\text{bio}} - \Psi_{\text{air}})}{\Psi_{\text{air}}} \right) \times 100 \right] \tag{3}$$

where  $\Psi_{\text{air}}$  and  $\Psi_{\text{bio}}$  are the standards of drain current at the time nanogap is without biomolecule and with biomolecule respectively [20].

### 3.1 Variation of energy band diagram, potential and drain current by modulating the dielectric constant of neutral biological molecules:

Fig. 2(a) portrays the band graph of DL-DMG-TFET in ON state when neutral biomolecules are confined in the nanocavity zone. The assessment of relative permittivity is identical to  $K=1$  when there is no neutral biomolecule or air is accessible in the nanogap region. The band descending near the source-channel convergence under the tunneling region is the important task in setting of biomolecules development. The energy band diagram apparently is bent to the most exceptional when biomolecules having high dielectric constant are immobilized in the nanogap zone. In any case, when no biomolecules are confined in the nanogap (suggests the change in relative permittivity from higher to unity) the band curve moves descending, which achieves an increase in barrier width across the source channel interface. [21]. Fig. 2(b) displays the varieties in potential of the DL-DMG-TFET in ON state when neutral biological molecules are confined inside the nanogap zone. In the energy band curve at tunneling junction intersection, the bands are seen to be contorted descending when neutral biological molecules are confined in the nanogap area close to the source-channel junction.

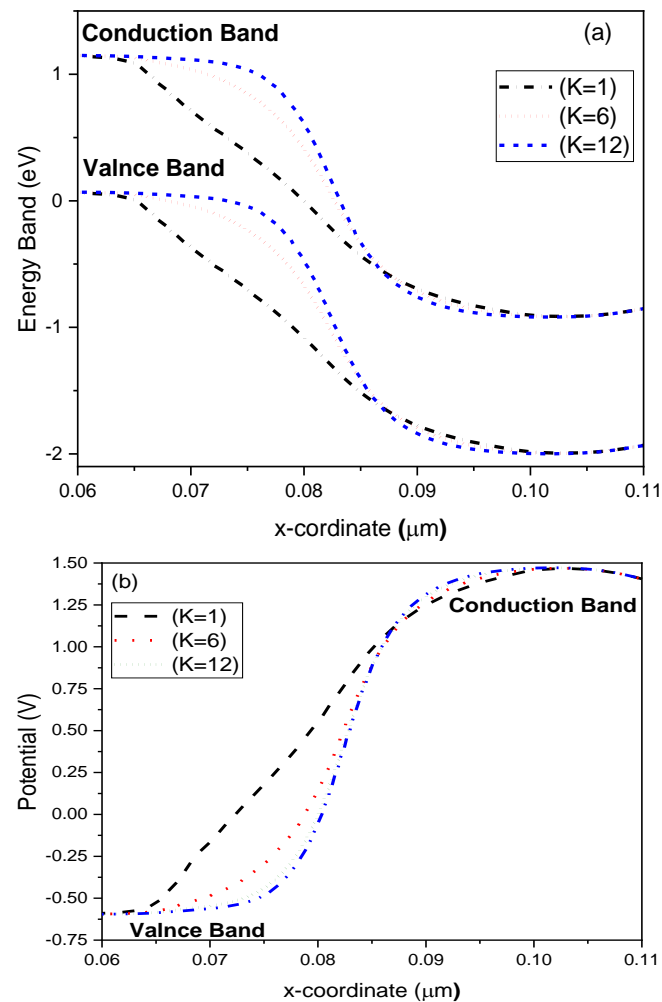


Fig.2. (a) Energy band diagram, and (b) Potential along x-coordinate at changing relative permittivity ( $k = 1, 6, 12$ ) and  $N_f = 0$ .

To distinguish the reflection of the biomolecule (neutral) present in the nanogap on the drain current, the dielectric constants of the objective biomolecule in the nanogap is adjusted from  $K=1$  to different estimation of  $K$  identified the different biological molecules ( $k=6$  of Bacteriophage T7 and  $K=12$  of

Gelatin). The output attributes of the DL-DMG-TFET biological sensor at the cavity length of 7 nm in Figure 3(a) and its sensitivity in Figure 3(b) for the drain voltage  $V_{DS}=1V$  are plotted. It is considered that as biological molecules linked to higher dielectric constants are confined in the nanogap the corresponding ON current will increase. This is because the effective field impacts availed by the gate bias is augmented as the dielectric constant of the nanocavity increments which results in higher gate capacitive coupling through the nanogap to the channel [20]. The barrier width at tunneling junction decreases due to an increment in the field effects which origins higher band bending and thus high drain current is rendered [21].

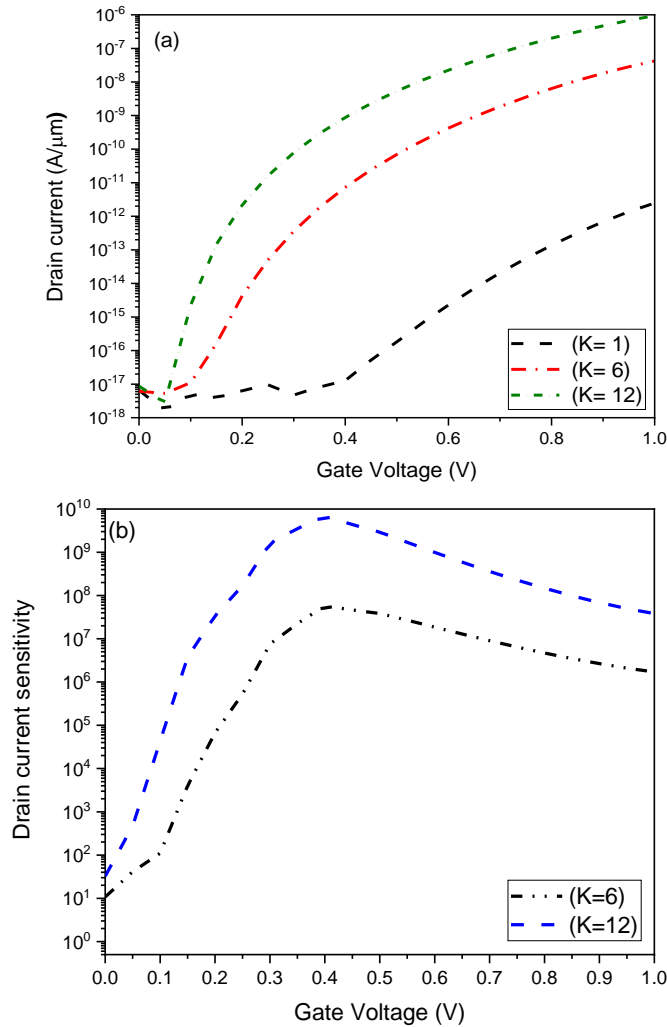


Fig.3. (a) ON Current improvement and (b) ON Current Sensitivity improvement, at different relative permittivity( $K = 1, 6, 12$ );  $N_f = 0$ ;  $T_{cav} = 2.5 \text{ nm}$ ; and  $L_{cav} = 7 \text{ nm}$ .

### 3.2 Impact of charged Biomolecules recognition on the DL-DMG-TFET biosensor potential and drain Current

The variation in potential is observed in Fig 4 when charged biomolecules are confined in the nanocavity area in the occurrence of neutral biomolecules by varying the surface charge density i.e.,  $n_f = -5 \times 10^{12} \text{ to } 5 \times 10^{12} \text{ cm}^{-2}$ . When nanogap is overloaded with positively charged biomolecules, it is an increase in potential for DL-DMG-TFET as seen in Fig. 4, which is utilized for sensing the biomolecules. The reverse process takes place during negatively charged biological molecules. At the time when negatively charged biomolecules are confined, there occurs a rise in flat band voltage ( $V_{fb}$ ) in the nanogap region. This,

in turn, leads to a decline in potential in the nanogap area negatively because, in the energy band characteristic at tunnelling interface, the band energy is observed to be warped in descending direction when positively charged biomolecules are confined in nanogap region near source channel intersection.

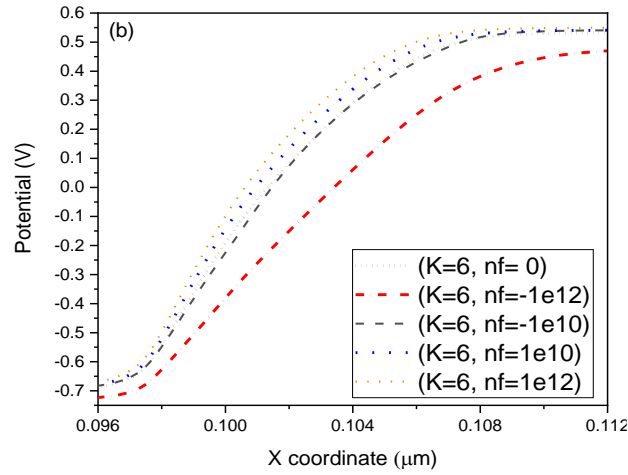


Fig. 4. Potential outcome for positively and negatively charged biomolecules at  $V_{DS} = 1 V$ .

With increments in potential, the tunneling probability increases at the interface of tunneling junction and  $I_D$  increments. Fig. 5(a and b) show drain current outcomes along with Gate voltage for negatively and positively charged biological molecules, respectively.

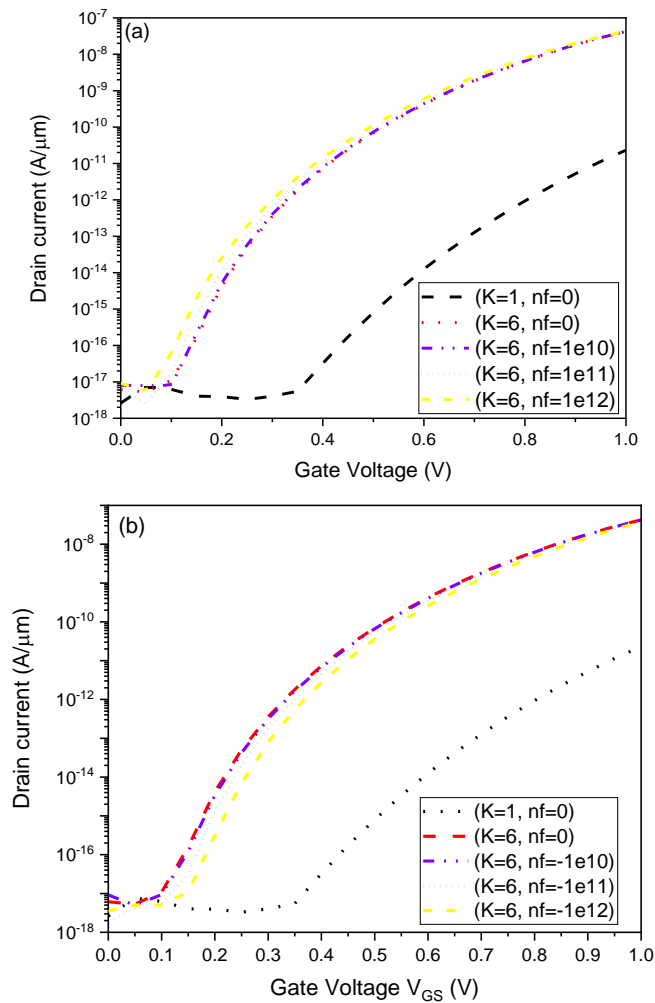


Fig. 5.  $I_D$ - $V_{GS}$  characteristics for (a) Positive and (b) Negative charged biological molecules  $V_{DS} = 1 V$ .

### 3.3 Effect of change in Device Geometric Parameters on Sensitivity:

Geometry parameters of structure such as nanogap region length ( $L_{cavity}$ ), Spacer Length ( $L_{us}$ ) and cavity thickness ( $T_{cav}$ ) is a key parameter for analysing the ON current characteristics of DL-DMG-TFET structure.

### 3.4 Impact of Cavity length ( $L_{cav}$ ) Variation:

The length of the nanogap area ( $L_{cavity}$ ) is a vital parametric variety for investigating the detecting characteristics of the device structure. In Figure 7a, it is seen that as the nanogap length is increasing from 7-10 nm fairly great execution regarding ON current is recorded. There is a large variation in ON current sensitivity as portrayed in Fig 7b because of variety in cavity length. This is on the grounds that DL-DMG-TFET shows tunnelling mechanism rather than thermionic phenomenon in MOSFET.

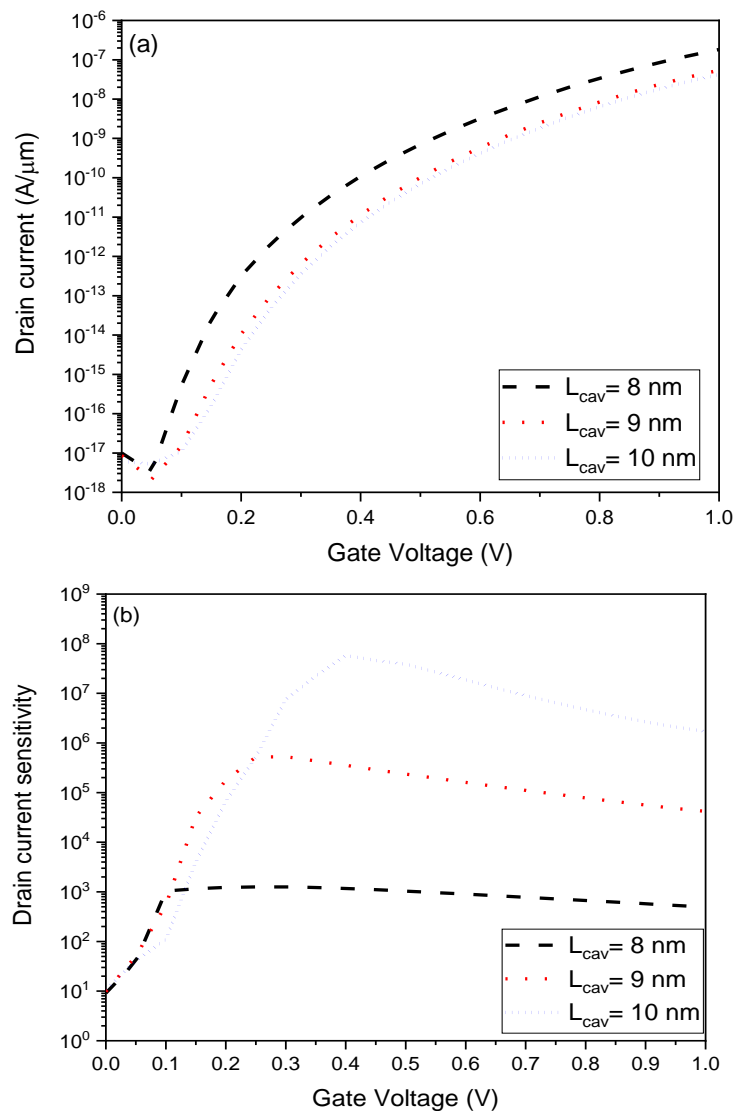


Fig. 7. (a)  $I_D$ - $V_{GS}$  characteristics for variation in cavity length ( $L_{cav}$ ) and (b) its sensitivity characteristics at  $V_{DS} = 1 V$ ,  $k = 5$ .



## 4 Conclusion

However, DL-DMG-TFET has higher affectability, specificity and sensitivity in biosensor application without augmentation of extra issues. The effects of a part of the basic assignments in a biosensor are seen a) fabrication problems, b) evaluation of biological sensors under dry and wet conditions. In DL-DMG-TFET structure, when there is an expansion in immobilization of biomolecules inside the cavity zone near the tunneling region. It prompts an increment in surface potential affectability and sensitivity for the proposed structure. In any case, DL-DMG-TFET devices are useful for recognition of biomolecules. Label free acknowledgement of biomolecules achieves higher sensitivity and affectability for neutral and charged biomolecules. Later on, DL-DMG-TFET devices can be used as a significantly delicate device for making ultrasensitive, low budget biomedical equipment by analyzing the impact of biomolecules on the electrical attributes of DL-DMG-TFET structure. It is seen that the proposed device has a low leakage current and has better affectability and sensitivity for charged biomolecules.

## References

- [1] S. Anand, S. I. Amin, and R. K. Sarin, "Performance Analysis of different material based Dual electrode doping-less TFET," *Eur. Adv. Mater. Congr.*, vol. 2, no. 6, pp. 384–387, Apr. 2017.
- [2] C. Sahu and J. Singh, "Charge-plasma based process variation immune junctionless transistor," *IEEE Electron Device Lett.*, vol. 35, no. 3, pp. 411–413, Mar. 2014.
- [3] Narang, R., Saxena, M. and Gupta, M., 2015. Drain current model of a four-gate dielectric modulated MOSFET for application as a biosensor. *IEEE Transactions on Electron Devices*, 62(8), pp.2636-2644.
- [4] Das, R., Chanda, M. and Sarkar, C.K., 2018. Analytical modeling of charge plasma-based optimized nanogap embedded surrounding gate MOSFET for label-free biosensing. *IEEE Transactions on Electron Devices*, 65(12), pp.5487-5493.
- [5] K.Na and Y. Kim, "Silicon complementary metal-oxide-semiconductor field-effect transistors with dual work function gate," *Japanese Journal of Applied Physics*, vol. 45, no.12, pp. 9033-9036, December 2006.
- [6] C.-W. Lee, A. Afzalian, N. D. Akhavan, R. Yan, I. Ferain, and J.-P. Colinge, "Junctionless multigate field-effect transistor," *Applied Physics Letters*, vol. 94, no. 5, pp. 053511-1–053511-2, February 2009.
- [7] Wei Long, Haijiang Ou, Jen-Min Kuo, and Ken K. Chin, "Dual-material gate (DMG) field effect transistor", *IEEE Transaction on Electron Devices*, vol. 46, no. 5, pp. 865-870, May 1999.
- [8] Tanu Wadhwa, Kakkar, D., Wadhwa, G., & Raj, B. (2019). Recent Advances and Progress in Development of the Field Effect Transistor Biosensor: A Review. *Journal of Electronic Materials*, 48(12), 7635-7646.
- [9] Tanu Wadhwa, Girish Wadhwa, Tarun Bhardwaj, Deepti Kakkar Balwinder Raj, "Design and Performance Analysis of Symmetrical and Asymmetrical Triple Gate Dopingless Vertical TFET for Biorecognition", *Silicon*, 1-9, 2020.
- [10] G. Wadhwa & B. Raj, "Label Free Detection of Biomolecules Using Charge-Plasma-Based Gate Underlap Dielectric Modulated Junctionless TFET". *Journal of Electronic Materials*, Vol.47. pp.4683-4693. 2018.
- [11] J. Tavakoli, and Y. Tang, "Hydrogel based sensors for biomedical applications: an updated review," *Polymers*, vol.9, 364.2017.
- [12] Y. C. Syu, W. E. Hsu, and C. T. Lin, "Field-Effect Transistor Biosensing: Devices and Clinical Applications," *ECS J Solid State Sci Technol*, vol. 7, pp.3196-3207.2018.
- [13] M. J. Kumar, and S. Janardhanan, "Doping-less tunnel field effect transistor: Design and investigation," *IEEE Trans. Electron Devices*, vol. 60, pp.3285-3290.2013.
- [14] G. Wadhwa, and B. Raj, "Parametric Variation Analysis of Symmetric Double Gate Charge Plasma JLTFTFET for Biosensor Application," *IEEE Sens. J.*, vol. 18, pp.6070-6077.2018.
- [15] "ATLAS User's Manual DEVICE SIMULATION SOFTWARE," 2004.
- [16] S. Kumar, and B. Raj, "Analysis of ION and Ambipolar Current for Dual-Material Gate-drain Overlapped DG-TFET," *J Nanoelectron Optoelectron*, vol. 11, pp.323-333.2016.
- [17] Kumar, P., Gupta, M. & Singh, K. Performance Analysis of Charge Plasma Based Five Layered Black Phosphorus-Silicon Heterostructure Tunnel Field Effect Transistor. *Silicon* 12, 2809–2817 (2020)
- [18] K. Zhuo, Y. Chen, L. Kang, S. Xu, and J. Wang, "Dielectric constants for binary amino acid– water solutions from (278.15 to 313.15) K," *J. Chem. Eng. Data*, vol. 54, pp.137-141.2008.
- [19] Wadhwa, G., Singh, J. and Raj, B., Design and investigation of doped triple metal double gate vertical TFET for performance enhancement. *Silicon*, pp.1-11, 2020.
- [20] Mahalaxmi, A. and Mishra, G.P., 2020. Performance Assessment of a Cavity on Source ChargePlasmaTFET-based Biosensor. *IEEE Sensors Journal*.
- [21] Wadhwa, G. and Raj, B., 2019. Design, Simulation and Performance Analysis of JLTFTFET Biosensor for High Sensitivity. *IEEE Transactions on Nanotechnology*, 18, pp.567-574.

- [22] Narang, R., Reddy, K.S., Saxena, M., Gupta, R.S. and Gupta, M., 2012. A dielectric-modulated tunnel-FET-based biosensor for label-free detection: Analytical modeling study and sensitivity analysis. *IEEE transactions on electron devices*, 59(10), pp.2809-2817.
- [23] M. Gholizadeh and S. E. Hosseini, "A 2-D analytical model for double gate tunnel FETs," *IEEE Trans. Electron Devices*, vol. 61, no. 5, pp. 1494–1500, May 2014, doi: 10.1109/TED.2014.2313037.
- [24] C. Wu, R. Huang, Q. Huang, C. Wang, J. Wang, and Y. Wang, "An analytical surface potential model accounting for the dual-modulation effects in tunnel FETs," *IEEE Trans. Electron Devices*, vol. 61, no. 8, pp. 2690–2696, Jun. 2014, doi: 10.1109/TED.2014.2329372.
- [25] J.-M. Choi, J.-W. Han, S.-J. Choi, and Y.-K. Choi, "Analytical modeling of a nanogap-embedded FET for application as a biosensor," *IEEE Transaction Electron Device*, vol. 57, no. 12, pp. 3477–3484, Dec. 2010. Rakhi Narang, Manoj Saxena, and Mridula Gupta, "Comparative Analysis of Dielectric-Modulated FET and TFET-Based Biosensor" *IEEE Transactions on Nanotechnology*, vol. 14, no. 3, pp. 427-435, May 2015.